



Article

Solid-Phase Extraction and Characterization of Quercetrin-Rich Fraction from *Melastoma malabathricum* Leaves

Mohd Azrie Awang ¹, Lee Suan Chua ^{2,3,*}  and Luqman Chuah Abdullah ⁴ 

¹ Faculty of Food Science and Nutrition, Universiti Malaysia Sabah, Jalan UMS, Kota Kinabalu 88400, Sabah, Malaysia

² Institute of Bioproduct Development, Universiti Teknologi Malaysia, Skudai, Johor Bahru 81310, Johor, Malaysia

³ Department of Bioprocess and Polymer Engineering, School of Chemical and Energy Engineering, Faculty of Engineering, Universiti Teknologi Malaysia, Skudai, Johor Bahru 81310, Johor, Malaysia

⁴ Institute of Tropical Forestry and Forest Products, Universiti Putra Malaysia, Serdang 43400, Selangor, Malaysia

* Correspondence: chualeesuan@utm.my or lschua@ibd.utm.my; Tel.: +60-197214378

Abstract: This study was focused on the recovery of quercetrin from the crude extract of *Melastoma malabathricum* leaves using the technique of solid-phase extraction. The process variables and their ranges were screened using one-factor-at-a-time and statistically optimized using the response surface methodology. The results found that 9.13 mg/mL of crude extract required 18.24 mL of 70.5% methanol as the eluent to yield an 86.6% *w/w* fraction containing 36.02 mg/g of quercetrin. The process increased quercetrin from 1% *w/w* in the crude extract to 4% *w/w* in the fraction. Quercetrin was likely to be the compound contributing to antiradical and antidiabetic activities. In silico simulation showed that quercetrin had low binding energy and mostly bound with charged (Glu and Arg) and aromatic (Tyr and Phe) amino acids via hydrogen bonds. Its inhibitory progress against DPP-IV was faster than crude extract at low concentration (<100 µg/mL).

Keywords: anti-diabetic; fractionation; optimization; quercetrin; solid-phase extraction



Citation: Awang, M.A.; Chua, L.S.; Abdullah, L.C. Solid-Phase Extraction and Characterization of Quercetrin-Rich Fraction from *Melastoma malabathricum* Leaves. *Separations* **2022**, *9*, 373. <https://doi.org/10.3390/separations9110373>

Academic Editor: Wojciech Piekoszewski

Received: 10 October 2022

Accepted: 14 November 2022

Published: 15 November 2022

Publisher's Note: MDPI stays neutral with regard to jurisdictional claims in published maps and institutional affiliations.



Copyright: © 2022 by the authors. Licensee MDPI, Basel, Switzerland. This article is an open access article distributed under the terms and conditions of the Creative Commons Attribution (CC BY) license (<https://creativecommons.org/licenses/by/4.0/>).

1. Introduction

Melastoma malabathricum, which is locally known as “senduduk”, is a small shrub belonging to the family Melastomaceae. This plant is native to the tropical and temperate regions in Asia, including Malaysia. The use of *M. malabathricum* as a medical herb is very popular amongst Malays and Indians. The leaves of *M. malabathricum* are usually chewed or pounded, and applied as a paste on the wounded area to stop bleeding [1]. According to Sharma et al. [2], the leaves could also be used to prevent scarring from smallpox, dysentery, diarrhea, and piles. The promising effects of the traditional application have encouraged studies on the chemical and biological activities of this plant nowadays.

Scientifically, *M. malabathricum* was prepared as extracts using different types of solvents and tested in various in vitro and in vivo studies to demonstrate its remarkable pharmacological potentials. The plant extracts, regardless of parts of the plant, were found to exhibit anti-inflammatory [1], antimicrobial [3], antioxidant [4], wound healing [5], antiulcer [6], anti-hyperlipidemic [7,8], and anti-diabetic [7–9] activities. However, most studies were focused on the biological activities of crude extract and limited information on the key phytochemical(s) contributing to the reported properties. Previously, quercetrin was reported to be one of the most abundant phytochemicals in *M. malabathricum* leaves [10]. Quercetrin is a glycosylated flavonol and quercetin is its basic chemical structure (Figure 1).

Fractionation is one of the herbal processing techniques to recover a target compound from a highly complex mixture of crude extract. There are two common fractionation techniques such as column chromatography and solid-phase extraction (SPE). The

preconcentration-extraction-based techniques are still in significant use to make analytes available for sensitive measurements [11]. Among them, SPE is also frequently used to preconcentrate the target compound from plant materials that has been reported in many studies [12,13]. A small quantity of target compound from a highly complex phytochemical composition of plant samples could be preconcentrated prior to analytical determination [14]. Many types of SPE sorbents are also available on the market, and therefore, the selection of sorbent is dependent upon its physical and chemical interaction with the analyte [15,16]. A reversed-phase C18 sorbent was found to be effective to isolate quercetin glycosides from plant-based samples [16,17]. SPE is widely used because it is a fast process with the minimal usage of solvent volume. The effectiveness of SPE was also dependent on the eluent system because its polarity would directly affect the interaction of the target compound and sorbent [18]. Methanol was used in the fractionation of quercetin glycosides, which possess intermediate polarity [16].

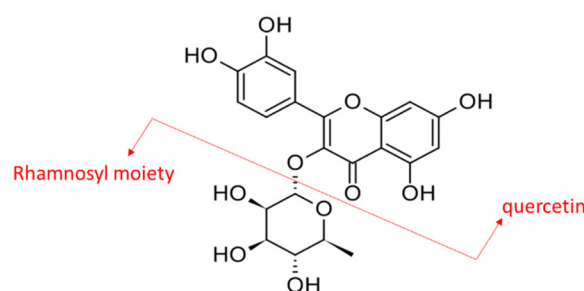


Figure 1. Chemical structure of quercetrin or quercetin O-glycoside composed of quercetin linked with a rhamnosyl moiety via a C3 glycosidic linkage.

The same group of researchers reported the preparation and optimization of crude extract from *M. malabathricum* leaves using ultrasound-assisted extraction. The yield of crude extract and quercetrin content was the dependent variables of the optimization [19]. Further investigation was carried out in the present study. Quercetrin was preconcentrated from the crude extract of *M. malabathricum* leaves using SPE. This SPE-based fractionation process was empirically and statistically optimized using the response surface methodology (RSM). To our knowledge, there were no studies on the optimization of quercetrin from *M. malabathricum* using RSM. However, there were studies carried out by a research team who used ultrasound-assisted solid-phase microextraction to preconcentrate quercetin (aglycone of quercetrin) from different vegetables and fruits, and the processes were optimized using the central composite design (CCD) of RSM [20,21].

In the present study, an empirical method, commonly known as one-factor-at-a-time (OFAT), is a single-factor experimental design, whereby one factor is varied at a time, while fixing other factors. Subsequently, statistical optimization was performed to depict the interaction effects among the input variables [22]. Both OFAT and RSM were used to optimize the independent variables such as the loading concentration of crude extract, volume of the eluent system, methanol concentration of the eluent system, and pressure of the manifold system to obtain a high yield of fraction and quercetrin content. The innovation of this article is to optimize the yield of quercetrin from *M. malabathricum* extract using both OFAT and RSM techniques, as quercetrin is one of the important phytochemicals with remarkable bioactivity of the herb. Process optimization would increase its yield for future bioproduct formulation and development. The antidiabetic property of quercetrin was also simulated *in silico* using the molecular docking approach and proven experimentally using a calorimetric DPP-IV assay.

2. Materials and Methods

The experimental works of this study can be divided into three phases: (i) ultrasound-assisted extraction for crude extract from *M. malabathricum* leaves, (ii) optimization of

solid-phase extraction for high yield of quercetrin, and (iii) characterization of recovered quercetrin. Figure 2 illustrates the overall flow of the research methodology.

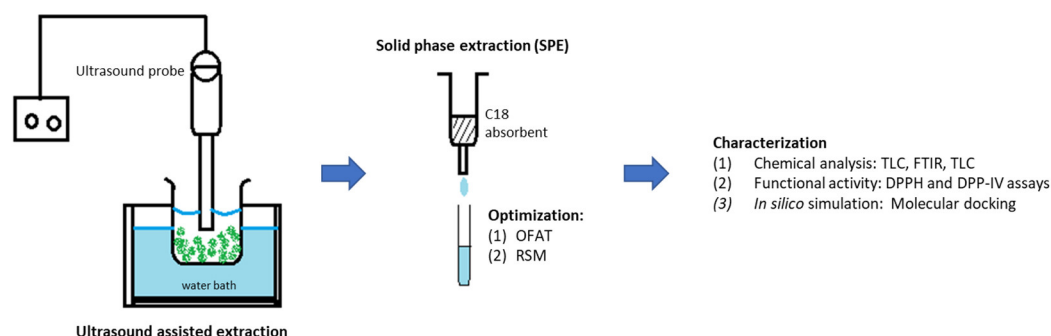


Figure 2. Schematic diagram of the experimental works.

2.1. Ultrasound-Assisted Extraction

The dried and ground leaves of *M. malabathricum* (10 g) were extracted in 210 mL of 70% ethanol for 15 min using an ultrasonic probe (Model FB-705, Newtown, CT, USA) operated at 68% amplitude as the optimized operating parameters in the works of Awang et al. [19]. The particle size of the dried leaves was 0.44–0.45 mm. The temperature of the ultrasound-assisted extraction system was maintained at 28 °C using a temperature-controlled water bath. The supernatant was filtered and dried in vacuo using a rotary evaporator.

2.2. Solid-Phase Extraction

The dried crude extract of *M. malabathricum* leaves was reconstituted in methanol (1 mL). The solution was loaded on a prepacked and activated reversed-phase cartridge, Chromabond C18 with the specification of 6 mL/500 mg × 45 µm (Macherey-Nagel, Allentown, PA, USA), for solid-phase extraction (SPE) to fractionate the crude extract into individual fractions. The activation was carried out by eluting the empty cartridge with 10 mL of deionized water followed by 10 mL of methanol. The activated cartridge was attached to a SPE vacuum manifold system. Fractionation was performed by slowly eluting the crude extract solution with an eluent system into tubes at a controlled flow rate under the stipulated pressure in the vacuum manifold system. The compound saturated eluent collected from the outlet of the cartridge was dried and determined for its fraction yield (weight %) and quercetrin content (mg/g), as presented in Equations (1) and (2), respectively.

$$\text{Yield (\% w/w)} = (\text{Mass of collected fraction}) / (\text{Mass of loaded crude extract}) \quad (1)$$

$$\text{Quercetrin (mg/g)} = (\text{Mass of quercetrin in the collected fraction (mg)}) / (\text{Mass of quercetrin in the loaded crude extract (g)}) \quad (2)$$

2.3. Preliminary Screening of Variables in Fractionation

Preliminary experiments were performed using the approach of One-Factor-At-A-Time (OFAT) to determine the range of independent variables such as loading concentration of crude extract (mg/mL), volume of eluent system (mL), methanol concentration (%), and pressure of the manifold system (kPa). Initially, the fractionation was carried out by varying the pressure from 15 to 30 kPa at the fixed loading concentration of crude extract (10 mg/mL) using 30 mL of 70% methanol as the eluent system. The optimum pressure was then selected and fixed at its value for subsequent experiments.

Consequently, the loading concentration of crude extract was varied from 3 to 25 mg/mL at the optimized pressure using 30 mL of 70% methanol. With the optimized pressure and loading concentration of crude extract, the fractionation process was continued using 30 mL of eluent with different concentrations of methanol ranging from 0 to 100% (v/v). Finally,

the crude extract solution was fractionated by varying the volume of the eluent system from 6 to 66 mL at the optimized pressure, the loading concentration of crude extract, and the methanol concentration. All experiments were conducted in triplicate. A new cartridge was used for each experiment.

2.4. Optimization of Fractionation for Crude Extract

The variables and their ranges were selected based on the results of OFAT screening for further statistical optimization. The selected variables were methanol concentration, loading concentration of crude extract, and volume of eluent system, which were optimized using the central composite design of the response surface methodology in Design-Expert Version 6.0.4 (Stat-Ease, Inc., Minneapolis, MN, USA). Three level factors of the experimental design produced a total of 17 experiments with three center points for the estimation of curvature and pure error (Table 1).

Table 1. Central composite design for 17 experiments performed at different ratios of eluent system, loading concentrations of crude extract, and numbers of cycles to fractionate plant crude extract.

Run of Experiments	Variables		
	Ratio of Eluent System (%)	Loading Concentration of Crude Extract (mg/mL)	Volume of Eluent Expressed in Cycle (1 cycle = 6 mL)
	A	B	C
1	55	10	4
2	10	15	1
3	10	5	1
4	55	18	4
5	55	1	4
6	100	10	4
7	10	15	7
8	55	10	4
9	55	10	4
10	100	15	7
11	100	5	7
12	110	5	7
13	55	10	9
14	100	15	1
15	100	5	1
16	55	0	1
17	10	10	4

2.5. Chemical Characterization of Crude Extract and Fraction

Thin-layer chromatography (TLC) was used to qualitatively analyze the presence of quercetrin in the crude extract and fraction. A silica gel 60 F254-coated TLC plate (5 cm × 7.5 cm, 0.05 mm thickness) was used to separate compounds in samples. A small drop of the reconstituted crude extract and fraction (1 mg/mL) was spotted on the baseline, which was drawn 1 cm above the end of the plate. The standard quercetrin was used as the positive control. The spotted samples were also distanced about 1 cm away from each other. The plate was then put vertically in a solvent-saturated glass chamber. The solvent system used for compound separation consisted of ethyl acetate: glacial acetic acid: formic acid: toluene (20:3:3:5 v/v). The solvent system was slowly migrated up the plate by capillary action. The movement of the solvent would separate compounds along the plate. The separation was stopped before the solvent reached the other end of the plate. The plate was air-dried and visualized under UV light at 254 nm. The location of quercetrin on the plate was determined based on the retention factor (Rf), which explains the ratio of distance travelled by quercetrin and solvent. The retention factors (Rf) of quercetrin from the crude extract and fraction were determined using Equation (3).

$$R_f = (\text{distance travelled by quercetrin})/(\text{distance travelled by solvent}) \quad (3)$$

Fourier-Transform Infrared Spectroscopy (FT-IR) was used to analyze the functional groups of quercetrin in samples. A 1 mg/mL sample was placed and pressed on the germanium disk with a constant pressure. Spectra were recorded with the aid of an OMNI-sampler using attenuated total reflectance (ATR). The absorbance was measured at wavenumbers ranging from 4000 cm^{-1} to 675 cm^{-1} .

Consequently, the quantitative analysis of quercetrin was determined using High-performance liquid chromatography (HPLC). A Waters HPLC system (Model 2690, MA, USA) consisted of a binary pump, a system controller, an automatic sampler, and a photodiode array detector (Model 966, MA, USA), which was used to separate compounds chromatographically. The column was a C18 reversed-phase column with dimensions of 4.6 mm \times 250 mm, 5 μm (Phenomenex, Torrance, CA, USA). The mobile phase that was composed of methanol: acetonitrile: water (40:15:45, $v/v/v$) with 1.0% acetic acid was flowed in isocratic elution. The flow rate of mobile phase was 1.0 mL/min and the injection volume was 10 μL . Quercetrin (HWI Analytik GmbH, Rülzheim, Germany) was detected at 368 nm.

2.6. Antiradical Assay

The antiradical assay was carried out using the DPPH assay. Radical DPPH is a stable free radical in purple color. It is reduced to yellow complex when reacted with antioxidants. The assay was performed according to the procedures explained by Awang et al. [19]. The crude extract and fraction were reconstituted in methanol at the concentration of 0.5 mg/mL. A 4.0 mL sample and 1.0 mL DPPH reagent (0.1 mM) were mixed and incubated for 3 min at room temperature. The absorbance of the mixture was measured at 520 nm using a Lambda 2S spectrophotometer (Perkin Elmer, Waltham, MA, USA). The absorbances of the negative control (methanol) and positive control (Trolox) were recorded. All experiments were performed in triplicate. The percentage of inhibition is calculated as in Equation (4).

$$\text{Inhibition (\%)} = (AC - A)/AC \times 100 \quad (4)$$

where AC is the absorbance of the control and A is the absorbance of the sample.

2.7. Anti-Diabetic Activity Using Dipeptidyl Peptidase-IV (DPP-IV)

Antidiabetic assay was carried out using DPP-IV kits. The assay measured the inhibition of DPP-IV after being treated with 1 mg/mL of crude extract and fraction. The progress of the inhibition was then monitored at different concentrations of samples (0–100 $\mu\text{g/mL}$). DPP-IV was used to cleave the nonfluorescent substrate, H-glycyl-prolyl-AMC, to form fluorescent product, 7-amino-4-methyl coumarin (AMC), for measurement at 405 nm. One unit of DPP-IV is the amount of enzyme required to yield 1.0 μmole of AMC per minute at 37 $^{\circ}\text{C}$ [23]. The calibration curve of AMC was established from 0–50 mM. Sitagliptin was used as a positive control. All experiments were performed in triplicate. The inhibitory activity is expressed in percentage as calculated using Equation (4).

2.8. Simulation Using Molecular Docking

The activity of quercetrin as the DPP-IV inhibitor was evaluated *in silico* using Autodock (4.2) software. Free energy binding, the inhibition constant, and surface interaction were analyzed to determine the inhibitory activity of quercetrin as a ligand against DPP-IV (protein). Sitagliptin was used as a reference drug.

2.9. Statistical Analysis

The triplicate data were averaged and determined for their standard deviations, which were then plotted in figures as error bars. One-way ANOVA followed by a post hoc Tukey–Kramer test was used to compare the statistical significance of results at 95% confident level.

3. Results and Discussion

3.1. Effect of Pressure on the Fraction Yield and Quercetrin Content

OFAT screening was carried out prior to optimization. The preliminary screening was used to decide the variables and their ranges for statistical optimization. The optimization aimed to increase the yield of fraction with the highest content of quercetrin. The operating pressure of the SPE manifold system is one of the critical parameters in process optimization. Figure 3a clearly shows that fractionation could achieve the maximum yield (80.5%) and quercetrin content (28.48 mg/g) at 20 kPa. The content of quercetrin was significantly dropped when the pressure was lower or higher than the optimum value. The vacuum pressure between 15 and 20 kPa was to warrant an intensive interaction between the sample and sorbent, as well as to ensure reproducible flow rate [24]. Increasing the vacuum pressure more than 20 kPa to the small cartridge would promote a faster flow rate of eluent, which would result in poor separation [25]. Previous studies applied SPE to recover organic explosives from wastewater at a pressure ≤ 20 kPa [26]. Therefore, the flow rate should be well controlled at the optimum value to avoid zone spreading because of the slow flow rate [27].

3.2. Loading Concentration of Crude Extract on the Fraction Yield and Quercetrin Content

The screening results showed that the yield of fraction and quercetrin content were increased with the increase in sample loading from 3 to 10 mg/mL and declined from 10 to 25 mg/mL (Figure 3b). With the increase in sample loading, nonpolar substances from the crude extract might occupy the surface of the absorbent and create a hindrance for quercetrin to flow through the cartridge for collection. Hence, the quercetrin content was reduced in the collected fraction after the cartridge achieved saturation. It was also difficult to maintain the required flow rate of eluent at a high concentration of sample loading. Statistical analyses revealed that the yield of fraction was not significantly different between the loading concentration of 5 and 10 mg/mL, and the difference in quercetrin content was also not significant between 10 and 15 mg/mL of sample loading. Therefore, the sample loading would be statistically optimized between 5 and 15 mg/mL to confirm the optimum sample loading for quercetrin recovery.

3.3. Methanol Concentration of Eluent on the Fraction Yield and Quercetrin Content

The eluent composition was also found to affect the yield and quercetrin content in the collected fraction. Figure 3c shows a significant increment in fraction yield using the eluent system with the increased methanol concentration from 0 to 10% v/v. A further increase in methanol concentration did not significantly increase the yield of fraction. On the other hand, the quercetrin content was significantly increased with the use of 0 to 30% v/v methanol. There was no significant increment in quercetrin content after the concentration of methanol was increased more than 30% v/v. Therefore, the range of eluent composition from 10 to 100% v/v methanol was chosen for the subsequent study of optimization.

The eluent composition would affect the van der Waals interaction between the sorbent, mobile phase, and analyte from the crude extract. This would affect the quality of the fraction as different compounds would be recovered from the crude extract. Increasing the methanol concentration would decrease the polarity of the eluent system, and therefore, more relatively non-polar to semi-polar compounds including quercetrin would be eluted out from the SPE cartridge.

3.4. Eluent Volume on the Fraction Yield and Quercetrin Content

The volume of the eluent would cause a small difference in fraction yield between 69.3 and 87.6%, and 27.8 and 22.2 mg/mL for quercetrin content. A slight decrease in fraction yield and quercetrin content was observed after applying a large volume in eluent (>30 mL or >5 cycles) in the fractionation process (Figure 3d). The decrease in quercetrin could be explained by the elution of other substances from the crude extract, thus lowering the concentration of quercetrin in the fraction. The reversed-phase C18 SPE sorbent was

likely to be less selective for quercetrin [28]. However, there were studies that reported no significant change at high volume of solvent elution for the recovery of phenolic compounds [29]. Thus, the volume of eluent was set at the range of 6 to 42 mL (1 to 7 cycles) in the subsequent optimization.

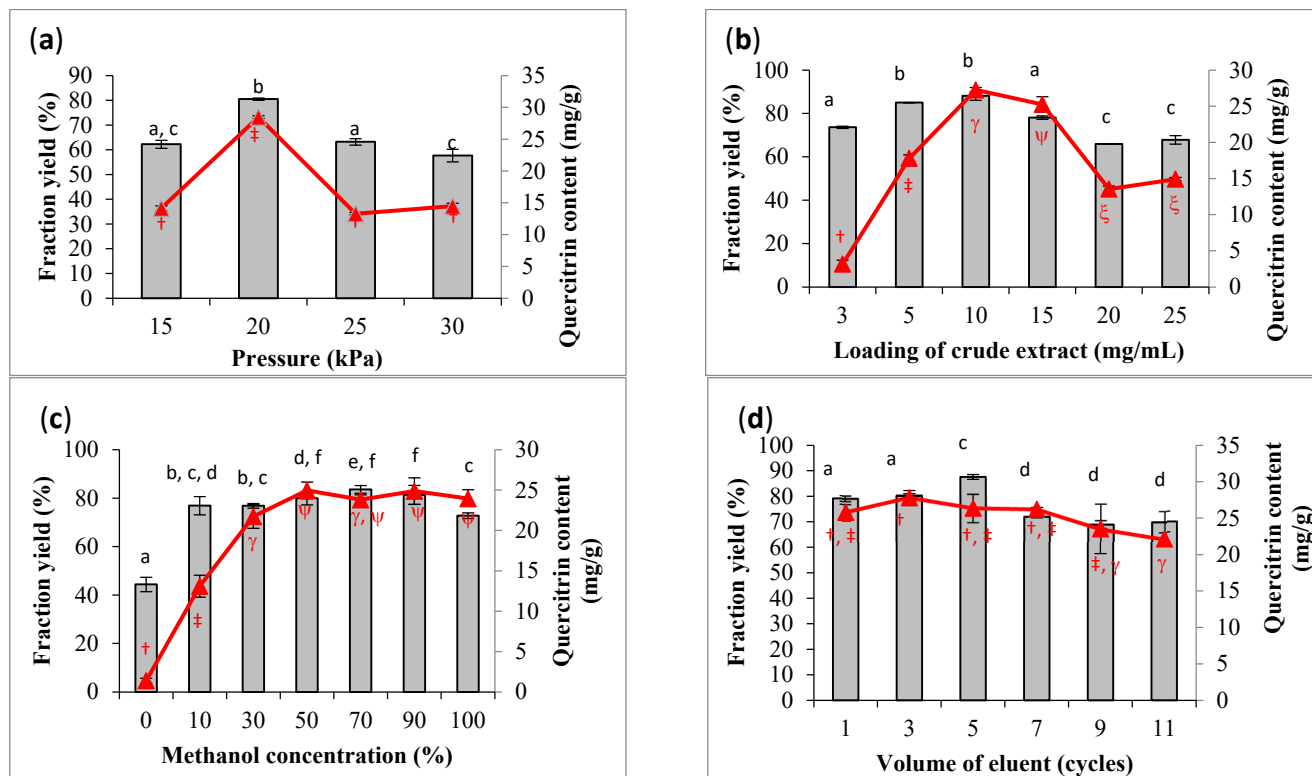


Figure 3. Screening parameters for high fraction yield (bar) and quercetrin content (line) based on one-factor-at-a-time (OFAT) approach. The screened parameters are (a) pressure (15–30 kPa), (b) loading concentration of crude extract (3–25 mg/mL), (c) methanol concentration (0–100%), and (d) volume of eluent expressed in number of cycles (1–11). Results are expressed in mean ± standard deviation of triplicate data. The mean values are significantly different if they do not share the same letter (bar) or symbol (line).

Based on the findings of OFAT screening, the pressure of the SPE manifold was fixed at 20 kPa. The other variables such as sample loading (5–15 mg/mL), methanol concentration (10–100% v/v), and eluent volume (6–42 mL) would be statistically optimized in the defined range to obtain a high yield of fraction and quercetrin content from the crude extract of *M. malabathricum* leaves. Therefore, OFAT screening allows the selection of variables for further optimization at the narrower range. Sorting out significant response variables prior to statistical optimization would be more efficient than direct optimization at a wide range of variables. Even though such an approach of OFAT screening followed by response optimization would have a few more experimental runs, it could produce better results. Response optimization is good for tradeoffs among variables as they are interdependent.

3.5. Optimization for Fractionation of Crude Extract

CCD was used to optimize the independent variables of methanol concentration, loading concentration of crude extract, and eluent volume. The results found that quadratic models were the best fit models for both fraction yield and quercetrin content with high coefficient of determination ($R^2 > 0.96$) and low standard deviations (<4.0). A low predicted residual error sum of square (PRESS) was also observed among the suggested models. The addition of interaction terms in quadratic models did not reduce the adjusted R^2 significantly. The difference between R^2 and adjusted R^2 was small (<0.042). The adjusted

R² would be remarkably reduced compared to R², if an insignificant term was introduced to the model [30]. The difference in adjusted R² and predicted R² was also <0.13 to explain the goodness of the fit. Kassama et al. [31] mentioned that statistical parameters such as the significance of regression model, lack of fit, coefficient of determination (R²), and adjusted R² were sufficient to prove the adequacy and validity of a model. Table 2 explains the output of ANOVA for both dependent variables such as fraction yield and quercetrin content. The quadratic models were very significant with a *p*-value < 0.001. The table also explains that methanol concentration (A) was not a significant variable to influence the yield of fraction, but it significantly affected the quercetrin content in the collected fraction. The interaction of methanol concentration (A) and loading concentration (B), and methanol concentration (A) and eluent volume (C) did not have significant effects on the quercetrin content. Apparently, the quercetrin content appeared to be influenced by the volume of eluent used during fractionation.

Table 2. Summary results for analysis of variance for the optimization models of both fraction yield and quercetrin content.

Dependent Variable: Fraction Yield						
Source	Sum of Square	Degree of Freedom	Mean Square	F Value	p-Value	
Model	2124.58	9	236.06	23.07	0.0002	Significant
Methanol concentration (A)	52.02	1	52.02	5.08	0.0588	
Sample loading concentration (B)	490.03	1	490.03	47.88	0.0002	
Volume of eluent (C)	58.19	1	58.19	5.69	0.0486	
AB	231.00	1	231.00	22.57	0.0021	
AC	167.88	1	167.88	16.41	0.0049	
BC	115.31	1	115.31	11.27	0.0121	
A ²	98.50	1	98.50	9.63	0.0173	
B ²	565.68	1	565.68	55.28	0.0001	
C ²	734.07	1	734.07	71.73	<0.0001	
Residual	71.64	7	10.23			Not significant
Lack of fit	50.53	5	10.11	0.96	0.5822	
Pure error	21.11	2	10.55			
Dependent variable: quercetrin content						
Model	2166.15	9	240.68	35.90	<0.0001	Significant
Methanol concentration (A)	190.42	1	190.42	28.40	0.0011	
Sample loading concentration (B)	219.15	1	219.15	32.69	0.0007	
Volume of eluent (C)	557.82	1	557.82	83.20	<0.0001	
AB	8.15	1	8.15	1.22	0.3066	
AC	35.18	1	35.18	5.25	0.0558	
BC	52.56	1	52.56	7.84	0.0265	
A ²	742.63	1	742.63	110.77	<0.0001	
B ²	474.83	1	474.83	70.82	<0.0001	
C ²	515.48	1	515.48	76.89	<0.0001	
Residual	46.93	7	6.70			Not significant
Lack of fit	40.07	5	8.01	2.33	0.3266	
Pure error	6.87	2	3.43			

After omitting the insignificant variables, the quadratic models of the fraction yield and quercetrin content can be described as Equations (5) and (6). The response surfaces in relation with the independent variables can be viewed in two-dimensional diagrams, as shown in Figure 4. The increase in methanol concentration in the eluent system (A) would increase quercetrin content, but not significantly affect the fraction yield. The loading concentration of crude extract (B) would positively affect the fraction yield and quercetrin content. High quercetrin content could be recovered if a higher crude extract was

loaded onto the column for fractionation. The increase in eluent volume would elute more compounds into the fraction, thus increasing the fraction yield. The negative coefficient of eluent volume (C) explains its inverse relationship with the quercetrin content as the fraction contained other substances, in addition to quercetrin.

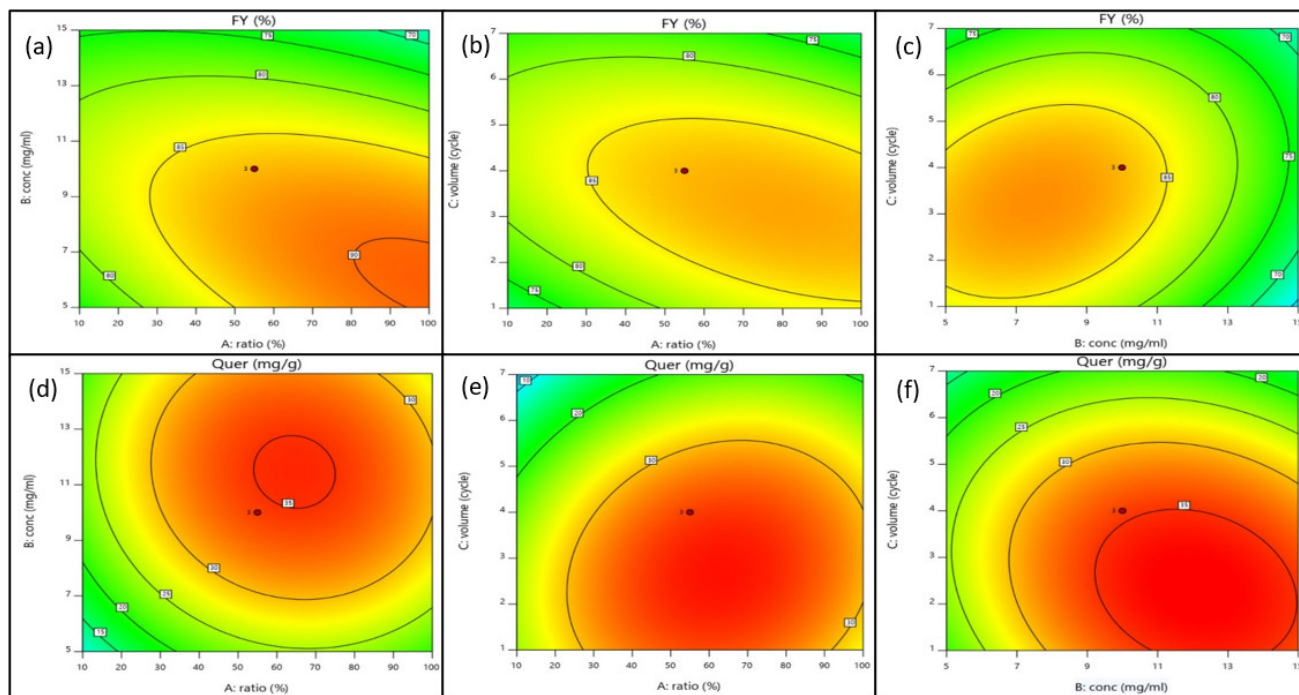


Figure 4. Two-dimensional contour plots of fraction yield (%) and quercetrin content (mg/g) resulting from the interactive effects of independent variables such as methanol concentration (A), loading concentration of crude extract (B), and volume of eluent expressed in cycle (C). (a) Contour plot of fraction yield resulting from the interaction of methanol concentration (A) and loading concentration of crude extract (B); (b) contour plot of fraction yield resulting from the interaction of methanol concentration (A) and volume of eluent expressed in cycle (C); (c) contour plot of fraction yield resulting from the interaction of loading concentration of crude extract (B) and volume of eluent expressed in cycle (C); (d) contour plot of quercetrin content resulting from the interaction of methanol concentration (A) and loading concentration of crude extract (B); (e) contour plot of quercetrin content resulting from the interaction of methanol concentration (A) and volume of eluent expressed in cycle (C); (f) contour plot of quercetrin content resulting from the interaction of loading concentration of crude extract (B) and volume of eluent expressed in cycle (C).

The fraction yield was increased with the increase in sample loading at low methanol concentration. However, the fraction yield was decreased at high methanol concentration. Most probably, the crude extract contained polar compounds that were more effectively eluted by the polar eluent system (low methanol concentration). A similar interaction was also observed for the methanol concentration and eluent volume to produce a high yield of fraction. The fraction yield was found to correlate positively with the interactive term of sample loading and eluent volume (BC). However, the quercetrin content was decreased at high sample loading, and even the saturated SPE cartridge was eluting with a high volume of eluent. Quercetrin was likely blocked due to the mass transfer hindrance along the column. The studies revealed that SPE was reliable and likely for simultaneous extraction and determination for target compound concentration.

Fraction yield, % (Y1):

$$Y1 = 41.73 + 4.77 B + 5.82 C - 0.02 AB - 0.03 AC + 0.25 BC - 0.001 A^2 - 0.28 B^2 - 0.90 C^2 \quad (5)$$

Quercetrin content, mg/g (Y2):

$$Y_2 = -25.58 + 0.51 A + 6.92 B - 4.73 C - 0.17 BC - 0.004 A^2 - 0.25 B^2 - 0.75 C^2 \quad (6)$$

3.6. Verification of Suggested Models

The statistical optimization suggests the optimized values for the independent variables as listed in Table 3. With the optimal values, SPE could produce a high yield of quercetrin-rich fraction. The models were successfully verified because a good agreement between the experimental data and the model predicted values was achieved. There were only small errors, namely 2.7% for fraction yield and 3.1% for quercetrin content. Therefore, the quadratic models could be used to predict the recovery of quercetrin from the fractionation process using SPE.

Table 3. Verification of both fraction yield and quercetrin content using the model-predicted values and experimental data at the optimized independent variables.

Ratio of Eluent System (%)		70.5
Loading Concentration of Crude Extract (mg/mL)		9.13
Volume of Eluent (Cycles)		3.04
Fraction Yield (%)	Predicted	88.97
	Experimental	86.61 ± 2.93
	(%) Error	2.65
Quercetrin Content (mg/g)	Predicted	34.93
	Experimental	36.02 ± 1.51
	(%) Error	3.12

3.7. Chemical Characterization of Quercetrin-Rich Fraction

HPLC was used to quantify the concentration of quercetrin in the crude extract and its fraction. The chromatograms show that the peak of quercetrin is detected at 12.1 min (Figure 5). Quercetrin was recovered and concentrated in the fraction after clean up by the SPE cartridge. The result showed about 86.6% of quercetrin could be recovered from the crude extract of *M. malabthricum* leaves. The content of quercetrin was increased from 1% *w/w* in crude extract to 4% *w/w* in the fraction after SPE-based fractionation.

The presence of quercetrin in the fraction could also be proven by matching the detected functional groups to those of standard quercetrin (Figure 6). The spectrum clearly showed a good match of quercetrin-rich fraction to the spectrum of standard quercetrin, except the loss of a sharp band at 1740 cm^{-1} (C=O stretching). The loss was probably due to the strong hydrogen bonding with other constituents in the fraction. The existence of the hydrogen bonding could also be proven from the disappearance of a few bands at 1369.56 cm^{-1} (O-H bending) and 1230–1200 cm^{-1} (C-O stretching) from the fraction. The other functional groups of quercetrin included the broad band of O-H stretching at 3318.54 cm^{-1} , O-H bending at 1415.93 cm^{-1} , C-H stretching at 2943.89 cm^{-1} and 2832.48 cm^{-1} , C-H bending at 1449.33 cm^{-1} , C=C stretching at 1658.46 cm^{-1} , and C=C bending at 684.26 cm^{-1} . C-O stretching consisting of an aliphatic ether (1114.19 cm^{-1}) and a sharp alkyl aryl ether (1020.86 cm^{-1}) was also found in the fraction.

3.8. In Silico Simulation of Dipeptidylpeptidase-IV Docking

In silico simulation was performed to predict the antidiabetic property of quercetrin by molecular docking with DPP-IV. The results of the simulation are presented in Table 4. It is shown that quercetrin had comparable binding energy with sitagliptin. The difference in the binding energy was relatively small, explaining how quercetrin could be a potential lead for diabetic drug development. The low binding energy between the ligand (quercetrin) and target molecule (DPP-IV) explains the stronger interaction, thus promoting antidiabetic activity [32].

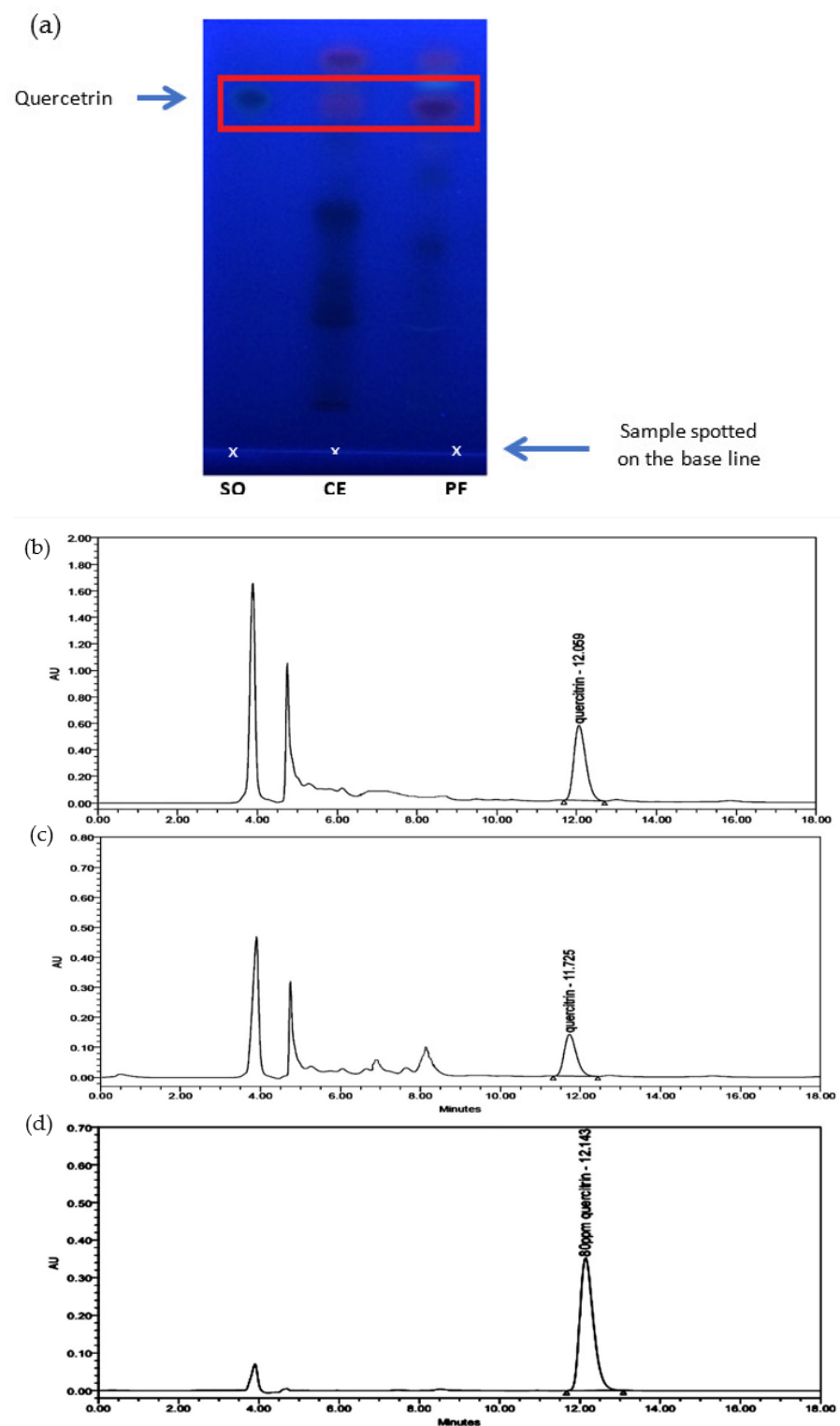


Figure 5. Detection of quercetrin in the crude extract and quercetrin-rich fraction prepared from *Melastoma malabathricum* leaves compared with standard quercetrin. (a) Thin-layer chromatogram spotted with standard quercetrin (SQ), crude extract (CE), and plant fraction (PF) on silica gel plate using the solvent system of ethyl acetate: glacial acetic acid: formic acid: toluene (20:3:3:5 *v/v*). HPLC chromatograms of (b) quercetrin-rich fraction, (c) crude extract, and (d) standard quercetrin separated by C18 column using the mobile phase of methanol: acetonitrile: water (40:15:45, *v/v/v*) with 1.0% acetic acid in isocratic elution.

Table 4. The binding energy and dissociation constant of quercitrin and sitagliptin acting as ligands to interact with amino acids.

Ligand	Type of Bonding	Interacted Amino Acids	Binding Energy (kcal/mol)	Dissociation Constant (K_d , μ M)
Quercitrin	Hydrogen	Glu202, Glu203, Arg354, Tyr586, Phe355	−6.21	46.14
	Electrostatic	Cys552		
	Hydrophobic	Ala358		
Sitagliptin	Hydrogen	Arg123, Arg307, Phe307	−8.45	0.64
	Electrostatic	Asp664, Glu203, Glu204, Tyr667		
	Hydrophobic	Tyr663, Tyr667, His741		

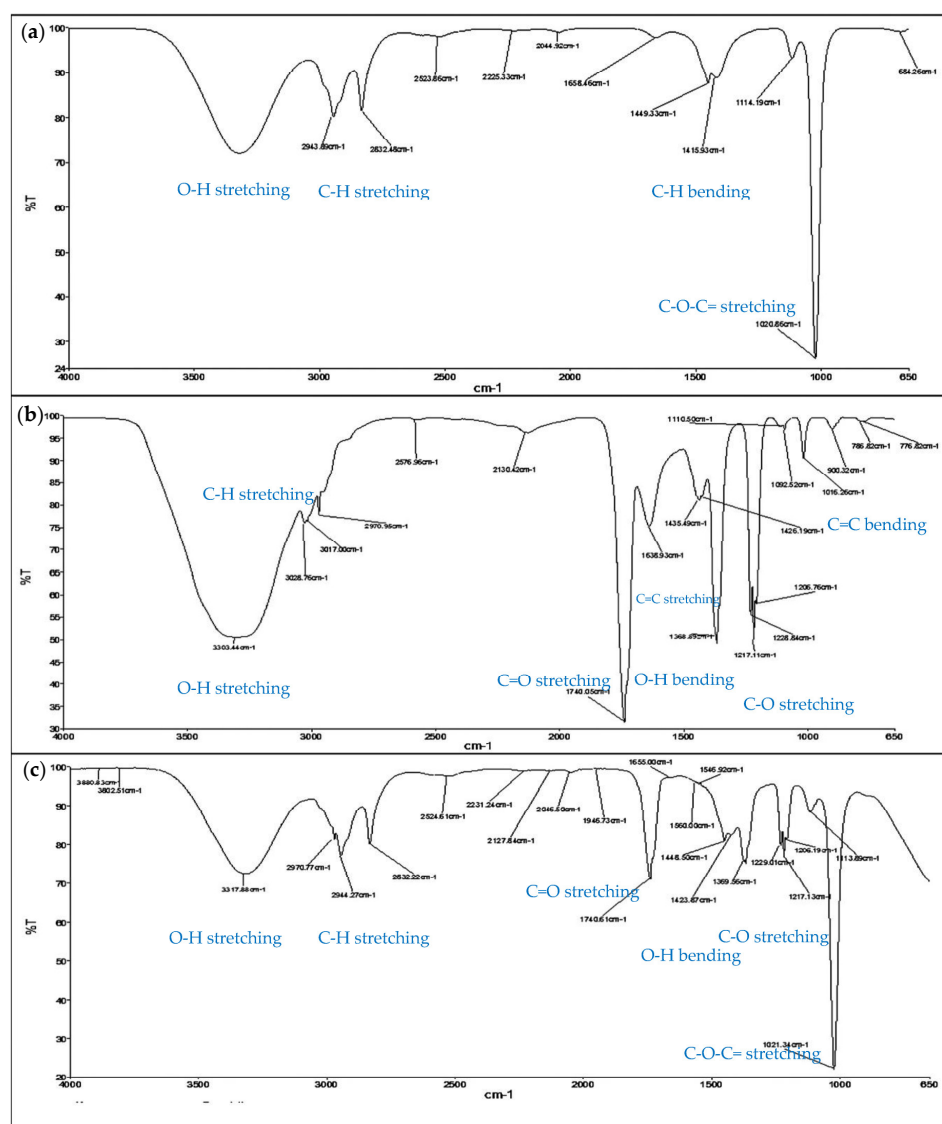


Figure 6. Identification of the functional groups of quercitrin detected in samples after extraction and fractionation using Fourier transform infrared spectroscopy (FTIR). The detection of functional groups is indicated in the FTIR spectra of (a) quercitrin-rich fraction, (b) crude extract, and (c) standard quercitrin for comparison.

Quercitrin was mostly interacting with the amino acid residues of DPP-IV by hydrogen bonding. The interacting amino acids were negatively charged glutamic acid, positively

charged arginine, and highly electronegative aromatic tyrosine and phenylalanine. This was because quercetrin is a glycosylated flavonol with the hydrophilic nature. On the other hand, sitagliptin interacted with the residues with electrostatic bonding as it had strong electronegativity due to the presence of fluorides in the molecular structure. Hence, the molecular action of quercetrin would be different from the inhibitory action exhibited by sitagliptin. The effectiveness of quercetrin to inhibit the active sites of DPP-IV and to exhibit the antidiabetic property was also experimentally proven in the calorimetric DPP-IV assay.

3.9. Anti-Diabetic Activity of Crude Extract and Fraction

The simulation was then experimentally validated using recombinant DPP-IV in a calorimetric assay. The inhibition of DPP-IV has been proven as an effective and safe therapy for the treatment of type II diabetes mellitus since the last decade [33,34]. The results showed that the antidiabetic property of *M. malabathricum* was mainly contributed by quercetrin and partly attributed to other plant constituents. This can be seen from Figure 7 in which the inhibition of fraction was not significantly different from standard quercetrin. The performance of crude extract was significantly higher than that of standard quercetrin, but not significantly different from that of the fraction.

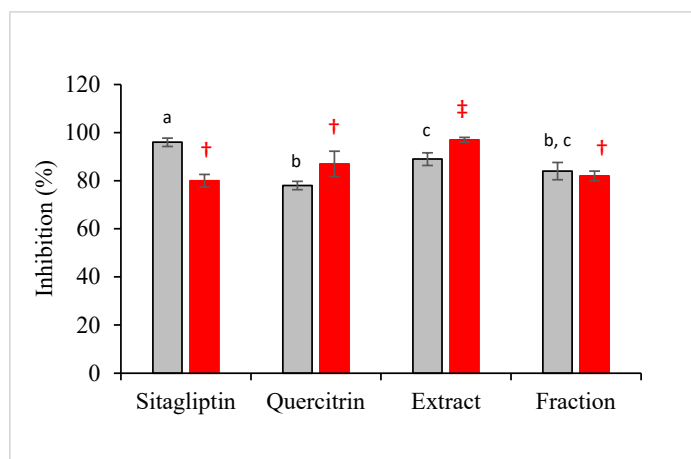


Figure 7. Antidiabetic (gray bar) and antioxidant (red bar) activities of sitagliptin (positive control), standard quercetrin, crude extract, and plant fraction expressed in inhibitory percentage. Results are expressed in mean \pm standard deviation of triplicate data. The mean values are significantly different if they do not share the same letter (antidiabetic) or symbol (antioxidant).

In the present study, the antioxidant capacity of samples based on the scavenging activity of radical DPPH was also performed. It is believed that the sample or compound with high antidiabetic property would also exhibit high antioxidative performance. Interestingly, the antioxidant activity of the fraction was not significantly different from the performance of standard quercetrin and standard drug, sitagliptin. Quercetrin that was successfully recovered from the crude extract of *M. malabathricum* would have a comparable performance with sitagliptin in quenching the radical chains.

Owing to the small difference in antidiabetic activities, all samples were prepared in different concentrations and monitored for inhibitory progress. A sharp increment in inhibitory action was observed for all samples at the concentration range from 0 to 60 $\mu\text{g/mL}$ (Figure 8). The inhibitory progress was slowed down after 60 $\mu\text{g/mL}$. Sitagliptin was found to have the highest increment in antidiabetic activity, whereas the crude extract showed the lowest increment in a concentration-dependent manner. The inhibitory progresses of standard quercetrin and fraction were almost similar at the lower range of concentration (<40 $\mu\text{g/mL}$). Obviously, the fraction could achieve higher performance than standard quercetrin at the concentration higher than 40 $\mu\text{g/mL}$.

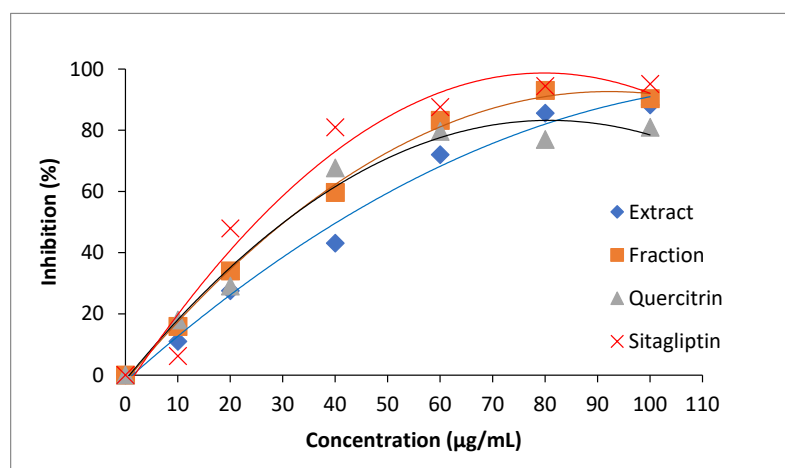


Figure 8. Inhibitory curves of dipeptidyl peptidase IV (DPP-IV) treated by crude extract (◆), plant fraction (■), standard quercetrin (▲), and sitagliptin (×).

In the subsequent experiments, the value of IC₅₀ was used to quantitatively compare the performance of samples. The lower IC₅₀ would provide higher antidiabetic activity because a lower concentration of the sample was required to achieve 50% DPP-IV inhibition. Therefore, the antidiabetic activity of crude extract, fraction, quercetrin, and sitagliptin was in ascending order as their IC₅₀ values were found to be 48.25 µg/mL, 30.71 µg/mL, 27.29 µg/mL, and 21.54 µg/mL, respectively. The inhibition of DPP-IV is known to relieve diabetic symptoms. The inhibition would decrease the fasting blood glucose level, increase insulin secretion, and improve oral glucose tolerance tests in animal studies [35]. The good performance of quercetrin is the antidiabetic property, most probably due to the presence of hydroxyl groups in the basic chemical structure [36]. Previously, Sarian et al. [37] also mentioned that the number of hydroxyl groups substantially influenced the activity of anti-diabetes.

4. Conclusions

M. malabathricum leaves were extracted by ultrasound-assisted extraction, and then the plant crude extract was further fractionated by a C18 reversed-phase SPE to concentrate quercetrin content. Ultrasound-assisted extraction was effective in leaching out many compounds from the plant leaves. The introduction of an additional SPE process aimed to remove undesirable plant polysaccharides in order to concentrate the quercetrin content in the plant fraction. The method is likely to be feasible and reliable to concentrate quercetrin from a highly complex mixture of natural product samples. OFAT screening followed by statistical optimization using the response surface methodology had successfully increased the content of quercetrin in the plant fraction from SPE. The fractionation technique of SPE was able to prepare a high yield of quercetrin-rich fraction (86.6%) with the quercetrin concentration up to 36.02 mg/g of fraction. The fraction possessed a high radical scavenging activity, which was more than 80% at 0.5 mg/mL of fraction, while its antidiabetic property could achieve up to 90% inhibition against DPP-IV at the concentration of 100 µg/mL. Quercetrin inhibited DPP-IV, mostly through hydrogen bonding with its amino acids. The inhibition of DPP-IV is the current strategy to discover a potent lead for the treatment of type 2 diabetes. Therefore, quercetrin is a highly potential phytochemical to be developed into a natural DPP-IV inhibitor. The future aim of the study is to use the optimized extraction variables to upscale the process for a high yield of quercetrin, mainly because of its promising antidiabetic property.

Author Contributions: Conceptualization, M.A.A. and L.S.C.; methodology, M.A.A.; software, L.C.A.; validation, M.A.A., L.S.C. and L.C.A.; formal analysis, M.A.A.; investigation, M.A.A.; resources, L.S.C.; data curation, L.C.A.; writing—original draft preparation, M.A.A.; writing—review

and editing, L.S.C.; visualization, L.C.A.; supervision, L.S.C.; project administration, L.S.C.; funding acquisition, L.S.C. All authors have read and agreed to the published version of the manuscript.

Funding: This research was funded by UNIVERSITI TEKNOLOGI MALAYSIA, grant number UTMHR-08G84.

Data Availability Statement: Not applicable.

Conflicts of Interest: The authors declare no conflict of interest. The funders had no role in the design of the study; in the collection, analyses, or interpretation of data; in the writing of the manuscript; or in the decision to publish the results.

References

1. Zakaria, Z.A.; Raden Mohd Nor, R.N.; Hanan Kumar, G.; Abdul Ghani, Z.D.; Sulaiman, M.R.; Rathna Devi, G.; Mat Jais, A.M.; Somchit, M.N.; Fatimah, C.A. Antinociceptive, antiinflammatory and antipyretic properties of *Melastoma malabathricum* leaves aqueous extract in experimental animals. *Can. J. Physiol. Pharmacol.* **2006**, *84*, 1291–1299. [\[CrossRef\]](#) [\[PubMed\]](#)
2. Sharma, H.K.; Chhangte, L.; Dolui, A.K. Traditional medicinal plants in Mizoram, India. *Fitoterapia* **2001**, *72*, 146–161. [\[CrossRef\]](#)
3. Johnny, L.; Yusuf, U.K.; Nulit, R. The effect of herbal plant extracts on the growth and sporulation of *Colletotrichum gloeosporioides*. *J. Appl. Biosci.* **2010**, *34*, 2218–2224.
4. Susanti, D.; Sirat, H.M.; Ahmad, F.; Ali, R.M. Bioactive constituents from the leaves of *Melastoma malabathricum* L. *J. Ilm. Farm.* **2008**, *5*, 1–8.
5. Anbu, J.; Jisha, P.; Varatharajan, R.; Muthappan, M. Antibacterial and wound healing activities of *Melastoma malabathricum* Linn. *Afr. J. Infect. Dis.* **2008**, *2*, 68–73. [\[CrossRef\]](#)
6. Wan Zainulddin, W.N.; Zabidi, Z.; Kamisan, F.H.; Yahya, F.; Ismail, N.A.; Nor Shamsah Din, N.S.; Mamat, S.S.; Hassan, H.; Mohtarrudin, N.; Zakaria, Z.A. Anti-ulcer activity of the aqueous extract of *Melastoma malabathricum* L. leaf in rats. *Pak. J. Pharm. Sci.* **2016**, *29*, 35–38.
7. Kumar, V.; Ahmed, D.; Gupta, P.S.; Anwar, F.; Mujeeb, M. Anti-diabetic, anti-oxidant and anti-hyperlipidemic activities of *Melastoma malabathricum* Linn. leaves in streptozotocin induced diabetic rats. *BMC Complement. Altern. Med.* **2013**, *13*, 222. [\[CrossRef\]](#)
8. Balamurugan, K.; Nishanthini, A.; Mohan, V.R. Antidiabetic and antihyperlipidaemic activity of ethanol extract of *Melastoma malabathricum* Linn. leaf in alloxan induced diabetic rats. *Asian Pac. J. Trop. Biomed.* **2014**, *4*, S442–S448. [\[CrossRef\]](#)
9. Prayoga, G.R.; Huda, A.S.; Br Sitepu, S.; Husnawati. The potency of Senggani (*Melastoma malabathricum* L.) leaves in repair of pancreatic beta cells for diabetes mellitus patients: A narrative review. *Curr. Biochem.* **2020**, *7*, 61–70. [\[CrossRef\]](#)
10. Nazlina, I.; Norha, S.; Noor Zarina, A.W.; Ahmad, I.B. Cytotoxicity and antiviral activity of *Melastoma malabathricum* extracts. *Malaysian J. Appl. Biol.* **2008**, *37*, 53–55.
11. Alexovič, M.; Andruch, V.; Balogh, I.S.; Šandrejová, J. A single-valve sequential injection manifold (SV-SIA) for automation of air-assisted liquid-phase microextraction: Stopped flow spectrophotometric determination of chromium(VI). *Anal. Methods* **2013**, *5*, 2497–2502. [\[CrossRef\]](#)
12. Jeong, S.H.; Choi, E.Y.; Kim, J.; Lee, C.; Kang, J.; Cho, S.; Ko, K.Y. LC-ESI-MS/MS simultaneous analysis method coupled with cation-exchange solid-phase extraction for determination of pyrrolizidine alkaloids on five kinds of herbal medicines. *J. AOAC Int.* **2021**, *104*, 1514–1525. [\[CrossRef\]](#) [\[PubMed\]](#)
13. Zhang, Y.; Zou, X.L.; Wang, Y.L.; Gao, L.; Chou, G.X. Determining the levels of four phenylethanoid glycosides and five triterpene acids in Liuwei Dihuang capsule using solid phase extraction with HPLC-UV. *J. Anal. Methods Chem.* **2019**, *2019*, 7609438. [\[CrossRef\]](#) [\[PubMed\]](#)
14. Bisgin, A.T. Single and simultaneous solid-phase extraction and UV-Vis determination for monitoring E129, E133 and E110 in foodstuffs. *Iran J. Sci. Technol. Trans. Sci.* **2020**, *45*, 163–175. [\[CrossRef\]](#)
15. Ku, Y.R.; Liu, Y.C.; Lin, J.H. Solid-phase extraction and high performance liquid chromatographic analysis of prednisone adulterated in a foreign herbal medicine. *J. Food Drug Anal.* **2001**, *9*, 150–152. [\[CrossRef\]](#)
16. Shui, G.; Peng, L.L. An improved method for the analysis of major antioxidants of *Hibiscus esculentus* Linn. *J. Chrom. A* **2004**, *1048*, 17–24. [\[CrossRef\]](#)
17. Silva, B.M.; Andrade, P.; Seabra, R.M.; Ferreira, M.A. Determination of selected phenolic compounds in quince jams by solid-phase extraction and HPLC. *J. Liq. Chrom. Relat. Technol.* **2001**, *24*, 2861–2872. [\[CrossRef\]](#)
18. Lau, C.H.; Chua, L.S.; Lee, C.T.; Aziz, R. Fractionation of rosmarinic acid from crude extract of *Orthosiphon stamineus* by solid phase extraction. *J. Eng. Sci. Technol.* **2015**, *10*, 104–112.
19. Awang, M.A.; Chua, L.S.; Abdullah, L.C.; Pin, K.Y. Drying kinetics and optimization of quercetin extraction from *Melastoma malabathricum* leaves. *Chem. Eng. Technol.* **2021**, *44*, 1214–1220. [\[CrossRef\]](#)
20. Asfaram, A.; Ghaedi, M.; Javadian, H.; Goudarzi, A. Cu- and S-SnO₂ nanoparticles loaded on activated carbon for efficient ultrasound assisted dispersive μ SPE-spectrophotometric detection of quercetin in *Nasturtium officinale* extract and fruit juice samples: CCD-RSM design. *Ultrason. Sonochem.* **2018**, *47*, 1–9. [\[CrossRef\]](#)

21. Asfaram, A.; Arabi, M.; Ostovan, A.; Sadeghi, H.; Ghaedi, M. Simple and selective detection of quercetin in extracts of plants and food samples by dispersive-micro-solid phase extraction based on core-shell magnetic molecularly imprinted polymers. *New J. Chem.* **2018**, *42*, 16144–16153. [[CrossRef](#)]
22. Tasharrofi, N.; Adrangi, S.; Fazeli, M.; Rastegar, H.; Khoshayand, M.; Faramarzi, M. Optimization of chitinase production by *Bacillus pumilus* using plackett-burman design and response surface methodology. *Iran. J. Pharm. Res.* **2011**, *10*, 759–768. [[PubMed](#)]
23. Yogisha, S.; Raveesha, K.A. Dipeptidyl peptidase IV inhibitory activity of *Mangifera indica*. *J. Nat. Prod.* **2010**, *3*, 76–79.
24. Burckhardt, B.; Laeer, S. Sample preparation and extraction in small sample volumes suitable for pediatric clinical studies: Challenges, advances, and experiences of a bioanalytical HPLC-MS/MS method validation using enalapril and enalaprilat. *Int. J. Anal. Chem.* **2015**, *5*, 796249. [[CrossRef](#)] [[PubMed](#)]
25. Fetterolf, D.M. Column Chromatography. *J. Valid. Technol.* **2009**, *15*, 43–48.
26. Abdah, S.N.M.; Sarmidi, M.R.; Yaakob, H.; Ware, I. Fractionation of *Labisia pumila* using solid-phase extraction for extraction of gallic acid. *J. Teknol.* **2014**, *69*, 65–68.
27. Vitha, M.F. Chapter 1: Fundamentals of Chromatography. In *Chromatography: Principles and Instrumentation*, 1st ed.; John Wiley & Sons, Inc.: Hoboken, NJ, USA, 2017; pp. 1–60.
28. Dugheri, S.; Marrubini, G.; Mucci, N.; Cappelli, G.; Bonari, A.; Pompilio, I.; Trevisani, L.; Arcangeli, G. A review of micro-solid-phase extraction techniques and devices applied in sample pretreatment coupled with chromatographic analysis. *Acta Chrom.* **2021**, *33*, 99–111. [[CrossRef](#)]
29. Radojkovic, M.M.; Zekovic, Z.P.; Vidovic, S.S.; Kocar, D.D.; Maskovic, P.Z. Free radical scavenging activity and total phenolic and flavonoid contents of mulberry (*Morus* spp. L., Moraceae) extracts. *Hem. Ind.* **2012**, *6*, 547–553. [[CrossRef](#)]
30. Ahmed, T.; Rana, M.R.; Zzaman, W.; Ara, R.; Aziz, M.G. Optimization of substrate composition for pectinase production from Satkara (*Citrus macroptera*) peel using *Aspergillus niger*-ATCC 1640 in solid-state fermentation. *Heliyon* **2021**, *7*, e08133. [[CrossRef](#)]
31. Kassama, L.S.; Shi, J.; Mittal, G.S. Optimization of supercritical fluid extraction of lycopene from tomato skin with central composite rotatable design model. *Sep. Purif. Technol.* **2008**, *60*, 278–284. [[CrossRef](#)]
32. Purnomo, Y.; Soeatmadji, D.W.; Sumitro, S.B.; Widodo, M.A. Anti-diabetic potential of *Urena lobata* leaf extract through inhibition of dipeptidyl peptidase IV activity. *Asian Pac. J. Trop. Biomed.* **2015**, *5*, 645–649. [[CrossRef](#)]
33. Patel, B.D.; Bhadada, S.V.; Ghate, M.D. Design, synthesis and anti-diabetic activity of triazolotriazine derivatives as dipeptidyl peptidase-4 (DPP-4) inhibitors. *Bioorg. Chem.* **2017**, *72*, 345–358. [[CrossRef](#)] [[PubMed](#)]
34. Mak, W.Y.; Nagarajah, J.R.; Abdul Halim, H.; Ramadas, A.; Pauzi, Z.M.; Pee, L.T.; Jagan, N. Dipeptidyl Peptidase-4 inhibitors use in type II diabetic patients in a tertiary hospital. *J. Pharm. Policy Pract.* **2020**, *13*, 34. [[CrossRef](#)] [[PubMed](#)]
35. Leng, S.H.; Lu, F.E.; Xu, L.J. Therapeutic effects of berberine in impaired glucose tolerance rats and its influence on insulin secretion. *Acta Pharmacol. Sin.* **2004**, *25*, 496–502. [[PubMed](#)]
36. Fan, J.; Johnson, M.H.; Lila, M.A.; Yousef, G.; de Mejia, E.G. Berry and citrus phenolic compounds inhibit dipeptidyl peptidase IV: Implications in diabetes management. *Evid. Based Complement. Alternat. Med.* **2013**, *2013*, 479505. [[CrossRef](#)] [[PubMed](#)]
37. Sarian, M.N.; Ahmed, Q.U.; Mat So'ad, S.Z.; Alhassan, A.M.; Murugesu, S.; Perumal, V.; Syed Mohamad, S.N.A.; Khatib, A.; Latip, J. Antioxidant and antidiabetic effects of flavonoids: A structure-activity relationship based study. *Biomed. Res. Int.* **2017**, *2017*, 8386065. [[CrossRef](#)] [[PubMed](#)]